Journal of Renewable Materials

Tech Science Press

DOI: 10.32604/jrm.2023.027544

ARTICLE

# Influence of Bayer Red Mud on the Operational and Mechanical Characteristics of Composite Cement Mortar

**Cheng Hu[1,2], Weiheng Xiang[1,3,*], Ping Chen[2,3], Yi Yang[4,5], Libo Zhou[3], Jiufang Jiang[5], Shunkai Li[2,4], Yang Ming[1] and Qing Li[3]**

[1]Guangxi Key Laboratory of New Energy and Building Energy Saving, Guilin University of Technology, Guilin, 541004, China

[2]College of Civil and Architectural Engineering, Guilin University of Technology, Guilin, 541004, China

[3]Guangxi Engineering and Technology Center for Utilization of Industrial Waste Residue in Building Materials, Guilin University of Technology, Guilin, 541004, China

[4]Collaborative Innovation Center for Exploration of Nonferrous Metal Deposits and Efficient Utilization of Resources, Guilin University of Technology, Guilin, 541004, China

[5]Guangxi Postdoctoral Innovation Practice Base, Guangxi Yufeng Cement Group Company Limited, Liuzhou, 545008, China

[*]Corresponding Author: Weiheng Xiang. Email: 2021072@glut.edu.cn

Received: 03 November 2022 Accepted: 31 January 2023 Published: 31 October 2023

## ABSTRACT

The aim of this study is to enhance the value and utilization of red mud generated in the Bayer process by preparing composite cement mortars. The effects of two different types of Bayer red mud with varying physical and chemical characteristics on the fluidity, mechanical strength, mineral composition, and microstructure of the composite cement mortar were systematically evaluated. The results showed that the optimal addition of red mud A was 10 wt%, while it was 20 wt% for red mud B. The mechanical properties of the composite cement mortar met the standards for P·O42.5 cement. Furthermore, the composite mortar with the addition of red mud B showed higher flexural and compressive strengths compared to the composite mortar with red mud A. This improvement is attributed to the smaller particle size of red mud B, which filled the micro-pores and increased the compactness of the cement stone, as well as its higher content of $Na_2O$, $K_2O$, and other free alkalis, which resulted in more obvious alkali activation, accelerating the hydration of the active minerals in the slurry.

## KEYWORDS

Bayer red mud; composite cement mortar; fluidity; mechanical strength; microstructure

## 1 Introduction

Red mud is a solid waste generated during the production of alumina via the Bayer process, which is used by over 90% of aluminum factories. As a result, Bayer red mud represents a significant proportion of total red mud emissions. On average, 1 to 1.5 tons of red mud are produced for every ton of alumina [1]. Global red mud discharge exceeds 70 to 90 million tons annually, with an average utilization rate of less than 15% globally, and just 4% in China [2]. Currently, red mud is mainly managed through

stockpiling and landfilling, resulting in a cumulative stockpile of over 2.7 billion tons [3] and causing land saline-alkalization and groundwater pollution.

Researchers have been studying ways to increase the utilization and value of red mud [4,5], which contains recyclable metal elements such as iron and titanium. However, the technology for metal extraction remains in the research stage and faces challenges such as high cost and energy consumption [6]. Red mud can also be used to improve soil acidity and phosphorus fixation capacity, but demand for this application is limited [7]. Red mud can be used to make glass ceramics with desirable properties for use in decorative glass as well as wear-resistant and corrosive-resistant materials. However, high energy consumption and radioactivity issues hinder its widespread industrial use [8]. Some hydrated minerals such as β-$C_2S$, $C_3A$, and others are present in red mud [9,10], and these materials can enable red mud to partially replace cement in cement-based materials, making this application an effective way to increase the utilization and value of red mud at present.

Compared to red mud produced through the sintering process, Bayer red mud has fewer active minerals and higher alkalinity, resulting in a lower utilization rate in cement-based materials [11–13]. As a result, researchers have attempted to create composite cementitious materials using Bayer red mud as the starting material in recent years, exploring the impact of Bayer red mud on the properties and microstructure of the composite cementitious materials [14–16]. For instance, Romano et al. [17] found that the presence of soluble aluminates and sodium ions in Bayer red mud promotes the formation of hydrated calcium aluminate and sodium silicoaluminate hydrate. Yang et al. [18] discovered that incorporating less than 6 wt% Bayer red mud can improve the compressive strength of cement mortar through increased hardened paste compactness and reduced $Ca(OH)_2$ content. Xu et al. [19] prepared a cementitious binder with over 40 MPa by using Bayer red mud, phosphogypsum, and granulated blast furnace slag as the main ingredients.

However, the Bayer red mud produced by different aluminum factories varies in grain size, chemical composition, mineral content, and physical-chemical properties [20,21]. Currently, most studies only examine the impact of Bayer red mud from a single source on composite cementitious materials, with comparative studies of multiple sources of Bayer red mud rarely conducted [22,23]. This hinders large-scale applications of Bayer red mud in cement-based materials.

This study aims to address the problem by systematically investigating the particle size distribution, leaching solution alkalinity, and mineral composition of Bayer red mud from two sources. Composite mortars were created by using the two sources of Bayer red mud to replace 10–30 wt% of Portland cement P·O42.5. The impact of Bayer red mud on the performance, mechanical strength, hydration products, and morphology of the cement composite mortar was analyzed. The effects of the two sources of Bayer red mud on the properties and microstructure of the composite mortar were also compared. The results of the study will provide guidance for improving the utilization rate of Bayer red mud in cement-based materials.

## 2 Experimental

The cement used in this experiment was ordinary Portland cement P·O42.5 produced by Guangxi Guilin Conch Cement Co. Ltd. (China). The red mud used was sourced from Guangxi Huasheng New Materials Co. (China) and Guangxi Pingguo Aluminum Industry Co. (China), represented as “red mud A” and “red mud B,” respectively. The chemical composition of the raw materials used in the experiment is shown in Table 1.

**Table 1:** Chemical composition of the raw materials

| Raw materials | Chemical composition (wt%) | | | | | | | | |
|---|---|---|---|---|---|---|---|---|---|
| | $Fe_2O_3$ | $Al_2O_3$ | $TiO_2$ | $SiO_2$ | CaO | MgO | $Na_2O$ | $K_2O$ | Others |
| Cement | 3.714 | 5.639 | 0.300 | 24.759 | 60.245 | 0.878 | 0.159 | 0.704 | 3.602 |
| Red mud A | 57.509 | 22.039 | 7.463 | 6.803 | 0.964 | 0.059 | 3.788 | 0.064 | 1.311 |
| Red mud B | 30.577 | 20.386 | 7.798 | 13.486 | 15.821 | 0.327 | 9.146 | 0.194 | 2.235 |

The two types of Bayer red mud, dried at 80°C to constant weight and ground to pass through a 200-mesh sieve, were used to replace 0%, 10%, 15%, 20%, 25%, and 30% of ordinary Portland cement (P·O42.5) by mass. By maintaining a water-binder ratio of 0.5, neat composite cement pastes and composite cement mortars with a binder-sand ratio of 1:3 were prepared. The mix proportions for the composite cement mortars are presented in Table 2. First, the composite cement pastes and mortars were mixed uniformly using an electric blender, then molded into 40 mm × 40 mm × 160 mm prismatic bodies and 40 mm × 40 mm × 40 mm cube bodies in iron molds for 24-h curing at 22°C and 60% relative humidity. Finally, they were cured in a standard maintenance room with a temperature of 20°C and relative humidity of 92% until reaching the specified age.

**Table 2:** Mix proportions of the composite cement mortar

| Specimen No. | Cementitious material contents (wt%) | | | Binder-sand ratio | Water-binder ratio |
|---|---|---|---|---|---|
| | Cement | Red mud A | Red mud B | | |
| A0/B0 | 100 | 0 | 0 | 1:3 | 0.5 |
| A1 | 90 | 10 | 0 | 1:3 | 0.5 |
| A2 | 85 | 15 | 0 | 1:3 | 0.5 |
| A3 | 80 | 20 | 0 | 1:3 | 0.5 |
| A4 | 75 | 25 | 0 | 1:3 | 0.5 |
| A5 | 70 | 30 | 0 | 1:3 | 0.5 |
| B1 | 90 | 0 | 10 | 1:3 | 0.5 |
| B2 | 85 | 0 | 15 | 1:3 | 0.5 |
| B3 | 80 | 0 | 20 | 1:3 | 0.5 |
| B4 | 75 | 0 | 25 | 1:3 | 0.5 |
| B5 | 70 | 0 | 30 | 1:3 | 0.5 |

The chemical compositions of the raw materials were determined by using an X-ray fluorescence analyzer (PANalytical Axios, Holland). The density and specific surface area of the raw materials were tested according to Chinese standards GB/T 208-2014 and GB/T 8074-2008. The pH of the leaching solution for Bayer red mud was measured according to the Chinese standard GB/T 5085.1-2007. The leaching test was performed as follows: the Bayer red mud powders were mixed with deionized water in a 1:10 weight ratio and then shaken for 8 h using an oscillator. The mixture was allowed to settle for 16 h. After being filtered through a 0.45 um fiber filter, the pH value of the leaching solution was determined using an intelligent digital-display acidometer.

The fluidity of the composite cement mortar was measured according to the Chinese standard GB/T 2419-2005. The flexural and compressive strengths of the composite cement mortar were tested according to the Chinese standard 17671–1999 for three specimens of each mixture, and the average strength was obtained after 3 d, 7 d, and 28 d of curing. When the curing age was reached, the composite cement pastes and mortars were immersed in 92 vol% ethyl alcohol for 24 h to prevent hydration. Subsequently, the paste specimens were ground for mineral composition analysis performed using an X-ray powder diffractometer (XRD, Riguku Ultima IV, Japan). Furthermore, the microscopic morphology of the mortar specimens was observed using a field emission scanning electron microscope (FE-SEM, Hitachi S4800, Japan) operated at 25 kV.

## 3 Results and Discussion

### *3.1 Characteristics of Bayer Red Mud*

The particle size distributions of cement, red mud A, and red mud B are shown in Fig. 1. As depicted, the particle size of cement ranges mainly from 8.50 to 143.50 μm, while that of red mud A is mainly from 0.85 to 10.00 μm; red mud B's particle size ranges mainly from 0.83 to 6.5 μm. The density of cement was found to be 3.15 g/cm$^3$ and its specific surface area was 356.50 m$^2$/kg. Red mud A and B had densities of 3.49 g/cm$^3$ and 3.02 g/cm$^3$ and specific surface areas of 786.65 m$^2$/kg and 880.40 m$^2$/kg, respectively. The order of particle size distribution for the three raw materials is red mud B < red mud A < cement. This leads to the conclusion that the addition of fine-particle-sized red mud A and B can fill pores in mortar and improve the mechanical properties of cement-based materials [24].

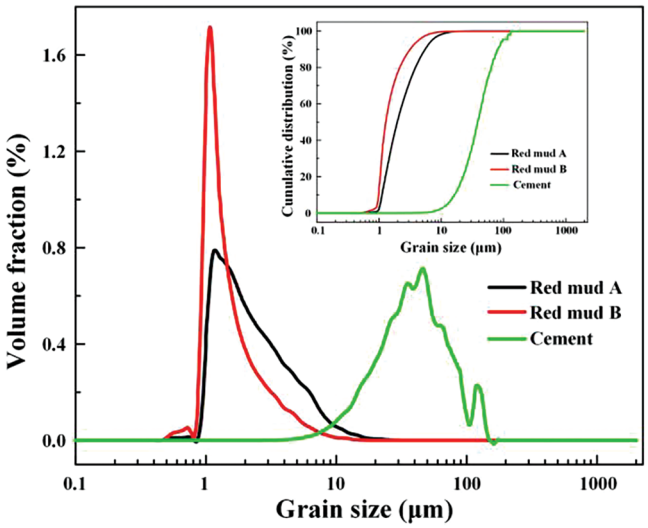


**Figure 1:** Particle size distributions of cement, red mud A, and red mud B

The pH values of the leaching solutions for red mud A and B are shown in Fig. 2. The pH values of the leaching solutions for both red mud A and B had minor fluctuations as leaching time increased, but stabilized after 7 h. The pH of the leaching solution for red mud A fluctuated between 10.05 and 10.50, whereas the leaching solution for red mud B fluctuated between 10.35 and 10.60. This suggests that red mud B has a higher content of free alkali compared to red mud A.

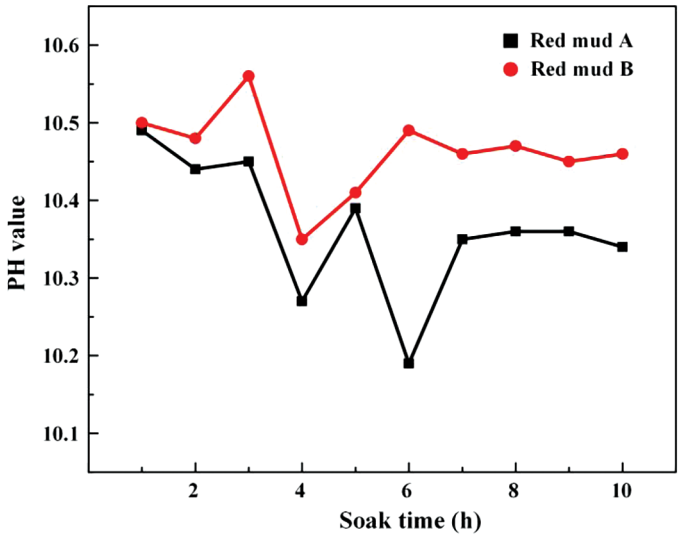


**Figure 2:** pH values of the leaching solutions for red mud A and B

The X-ray diffraction analysis results for raw red mud A and red mud B, after conducting calcination at various temperatures, are shown in Fig. 3. The main mineral components of red mud A and red mud B include: hematite ($Fe_2O_3$), perovskite ($CaTiO_3$), rutile ($TiO_2$), hibschite ($Ca_3Al_2Si_2O_{10}{\cdot}H_2O$), diaspore ($Al_2O_3{\cdot}H_2O$), quartz ($SiO_2$), grossular ($Ca_3Al_2Si_3O_{12}$), and cancrinite ($Na_6Ca_2Al_6Si_6O_{24}$ $(CO_3)_2{\cdot}2H_2O$), among others.

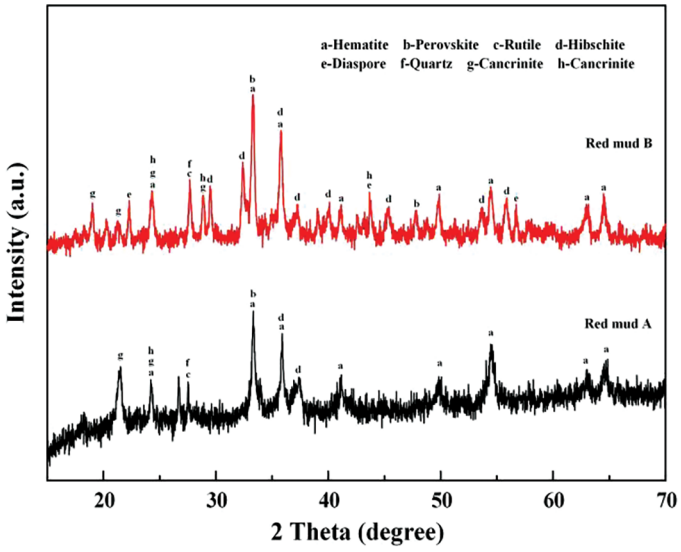


**Figure 3:** X-ray diffraction analysis of raw red mud A and red mud B

### *3.2 Properties and Microstructure of the Composite Cementitious Materials*

The effect of adding red mud A and red mud B on the flowability of cement mortar is shown in Fig. 4. It was found that the fluidity of pure cement mortar was 225.0 mm. However, as the amount of red mud A or

red mud B increased, the fluidity of the composite cement mortar gradually decreased. This is attributed to red mud's high specific surface area, which absorbs some of the free water during the mortar preparation process and causes a thickening effect, reducing the composite cement mortar's working performance [25].

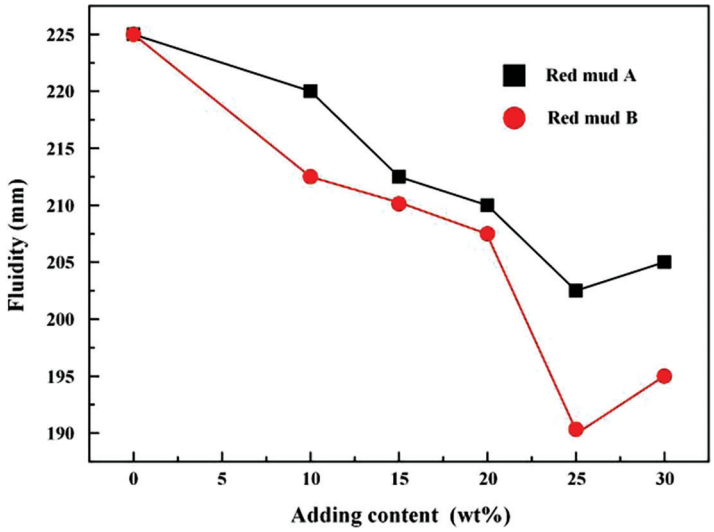


**Figure 4:** Impact of red mud A and red mud B on the flowability of cement mortar

Additionally, compared to red mud B, red mud A in the cementitious composite mortar had higher fluidity under the same admixture conditions. This is because red mud B had a larger specific surface area and absorbed more free water, leading to a greater decrease in the fluidity of cementitious composite mortar with red mud B.

As seen in Table 3, the initial setting time of composite mortar decreased as the amount of Bayer red mud increased, while the final setting time increased. This is because the free alkali in Bayer red mud raises the pH value of the cement mortar and promotes hydration of $C_3A$ and $C_4AF$, thus shortening the initial setting time. However, the hydration behavior of active minerals in Bayer red mud can consume parts of hydration product $Ca(OH)_2$, which delays the final setting time of the composite mortar to some extent.

**Table 3:** Operational properties and mechanical strength of the composite mortar

| Specimen No. | Fluidity/mm | Setting time/min | | Flexural strength/MPa | | | Compressive strength/MPa | | |
|---|---|---|---|---|---|---|---|---|---|
| | | Initial | Final | 3 d | 7 d | 28 d | 3 d | 7 d | 28 d |
| A0/B0 | 225.0 | 230 | 330 | 4.4 | 5.5 | 7.3 | 21.7 | 35.0 | 53.3 |
| A1 | 220.0 | 220 | 340 | 5.1 | 5.8 | 7.4 | 26.3 | 34.7 | 43.1 |
| A2 | 212.5 | 215 | 345 | 4.9 | 5.2 | 6.6 | 24.6 | 31.6 | 36.2 |
| A3 | 210.0 | 205 | 340 | 4.6 | 5.1 | 6.6 | 23.7 | 30.6 | 36.9 |
| A4 | 202.5 | 210 | 350 | 5.0 | 5.1 | 6.6 | 23.5 | 29.1 | 33.6 |
| A5 | 205.0 | 205 | 355 | 4.3 | 4.7 | 6.1 | 22.4 | 27.2 | 32.3 |
| B1 | 212.5 | 215 | 335 | 4.9 | 5.7 | 6.5 | 26.1 | 35.9 | 44.9 |

(Continued)

**Table 3 (continued)**

| Specimen No. | Fluidity/mm | Setting time/min | | Flexural strength/MPa | | | Compressive strength/MPa | | |
|---|---|---|---|---|---|---|---|---|---|
| | | Initial | Final | 3 d | 7 d | 28 d | 3 d | 7 d | 28 d |
| B2 | 210.0 | 210 | 345 | 4.3 | 5.9 | 7.2 | 26.2 | 35.5 | 46.2 |
| B3 | 207.5 | 205 | 350 | 4.9 | 5.3 | 7.4 | 27.5 | 34.5 | 43.3 |
| B4 | 190.5 | 195 | 355 | 4.6 | 6.4 | 7.4 | 26.9 | 34.8 | 42.2 |
| B5 | 195.0 | 200 | 360 | 3.9 | 4.8 | 6.6 | 23.9 | 33.3 | 39.8 |

Comparing the series A and series B specimens, series B had lower fluidity, a lower initial setting time, and a higher final setting time under the same conditions.

The impact of incorporating different amounts of red mud A on the mechanical strength of composite cement mortar is shown in Fig. 5. The results indicate that as the amount of red mud A increases, the 3-d, 7-d, and 28-d flexural strengths of the A series composite mortar specimens first increase and then decrease. Compared to the control specimen A0, the 3-d flexural strengths of specimens A1-A5 increased by 15.9%, 11.4%, 4.5%, 13.6%, and −2.2%, while the 28-d flexural strengths increased by 1.4%, −9.6%, −9.6%, −16.4%, and −17.8%, respectively.

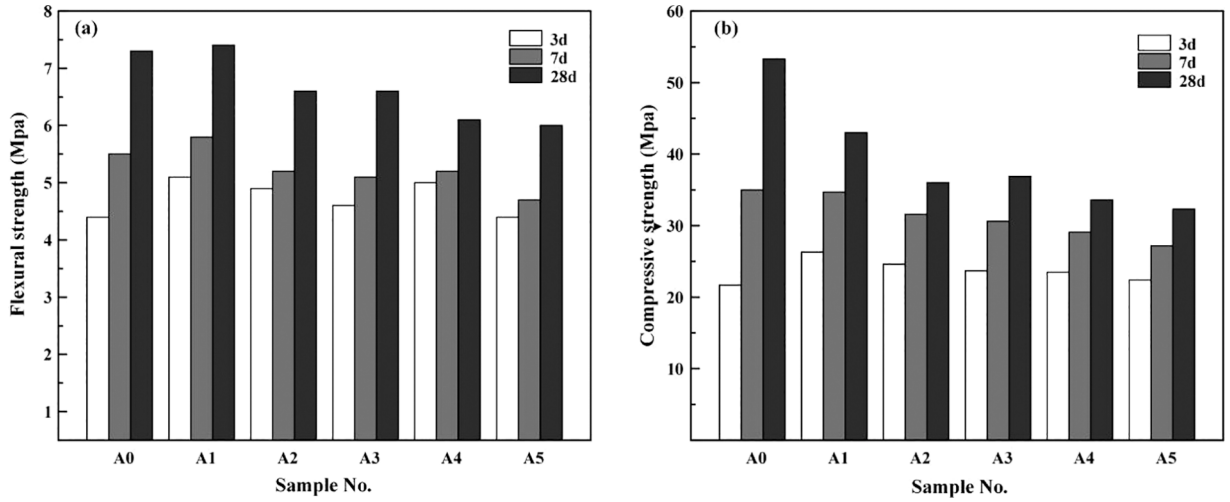


**Figure 5:** Effect of the amount of red mud A on the mechanical strength of composite cement mortar

The 3-d compressive strength of the A series specimens increased initially and then decreased with increasing amounts of red mud, while the 7-d and 28-d compressive strengths gradually decreased. In comparison to specimen A0, the 3-d compressive strengths of specimens A1-A5 increased by 21.2%, 13.4%, 9.2%, 8.3%, and 3.2%, and the 28-d compressive strengths increased by −19.1%, −32.1%, −30.8%, −37.0%, and −39.4%, respectively.

Therefore, it can be concluded that the optimal amount of red mud A for the composite cement mortar is 10%, at which point the red mud-cement composite mortar meets the strength requirements of P·O42.5 cement as specified in the Chinese standard GB 175-2007.

The effect of the amount of red mud B on the mechanical strength of the composite cement mortar is illustrated in Fig. 6. The 3-d, 7-d, and 28-d flexural strength values of the composite mortar specimens of the B series showed a trend of increasing and then decreasing with an increase in red mud B. When compared to the blank specimen B0, the 3-d flexural strengths of specimens B1–B5 increased by 11.4%, −2.3%, 11.4%, 4.5%, and −11.4%, respectively, while the 28-d flexural strengths increased by −11.0%, −1.4%, 1.4%, 1.4%, and −9.6%. The 3-d and 7-d compressive strength values of the series B specimens increased and then decreased with the incorporation of red mud B, while the 28-d compressive strengths showed a trend of gradually decreasing. Compared to the blank specimen B0, the 3-d compressive strength values of specimens B1-B5 increased by 20.3%, 20.7%, 26.7%, 24.0%, and 10.1%, respectively, and the 28-d compressive strength values increased by −15.8%, −13.3%, −18.8%, −20.8%, and −25.3%. The optimal amount of red mud B was determined to be 20%, at which point the red mud-cement composite mortar met the strength standards set by the P·O42.5 cement strength as specified in China's GB 175-2007 standard.

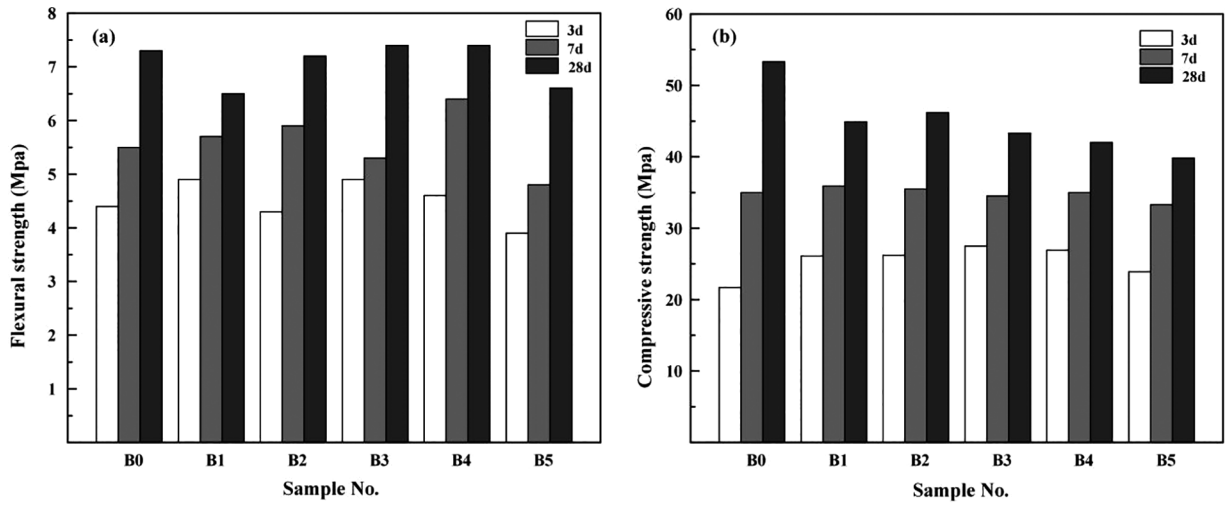


**Figure 6:** Effect of the amount of red mud B on the mechanical strength of composite cement mortar

Combining the research results, it was found that composite mortars with the addition of 10–25 wt% red mud A and B had higher mechanical strength compared to pure cement mortar at the curing age of 3 d. This is due to the favorable impact of the appropriate admixture of red mud on the early strength of the composite mortar. The reasons for this impact are [26–28]: (1) The small particle size of Bayer red mud fills the internal pores of the mortar, improving the compaction of hardened cement and enhancing its mechanical strength; (2) The free alkali in Bayer red mud, such as $Na^+$ and $K^+$, promotes the depolymerization of $SiO_4$ and $AlO_4$ in the composite cement mortar by alkali activation, inducing their repolymerization and forming a three-dimensional mesh-structured gel product. This accelerates early hydration, promoting the formation of hydration products, such as C- (A) S-H gel and AFt, and improving the 3-d flexural and compressive strength of the composite mortar; (3) The Bayer red mud has plenty of active Al and Si, which is beneficial for promoting the formation of C- (A) S-H gel. This gel has better mechanical properties than C-S-H gel, improving the strength of the composite mortar.

However, active minerals such as $C_3S$ and $C_2S$ were not found in red mud A and B according to XRD analysis results in Fig. 3. The Bayer red mud powders also had little hydration activity, as confirmed in previous literature [29,30]. Thus, the composite mortars with the incorporation of Bayer red mud had a lower increase in later strength. This made the 28-d flexural and compressive strengths of series A and B

specimens lower than those of the base group specimen B0. Excessive incorporation of Bayer red mud also led to a significant reduction in the compressive strength of the composite mortar at 28 d.

Additionally, it was found that the mechanical strength of series B specimens was higher than that of series A specimens when adding the same amount of Bayer red mud. This is because (1) the alkali content in red mud B was higher, providing a better alkali activation effect; (2) the particle size of red mud B was smaller, better filling the internal pores and improving the denseness of the composite cementitious mortar.

To study the impact of Bayer red mud on the mechanical properties of cement mortar, this study delved further into the effect of admixture of red mud B on the mineral composition of the composite mortar. The results are shown in Fig. 7. The main mineral compositions of the blank control group B0 and composite cement mortar specimens B1, B3, and B5 are $Ca(OH)_2$, $SiO_2$, $C_2S$, $C_3S$, AFt, and $CaCO_3$. $SiO_2$ appears due to the presence of quartz in Bayer red mud. After 7 d of curing, the peak intensity of the hydration product $Ca(OH)_2$ decreases as the amount of red mud B increases, as the active substances $Al_2O_3$ and $SiO_2$ in red mud consume part of $Ca(OH)_2$. At the curing age of 28 d, the peak intensity of the hydration product $CaCO_3$ increases with the increase of red mud B, due to the alkaline ions in red mud promoting the preliminary hydration reaction and producing more $CaCO_3$ as the curing age increases. At the same time, new peaks of single-carbon hydrated calcium aluminosilicate carbonate (AFm) are detected.

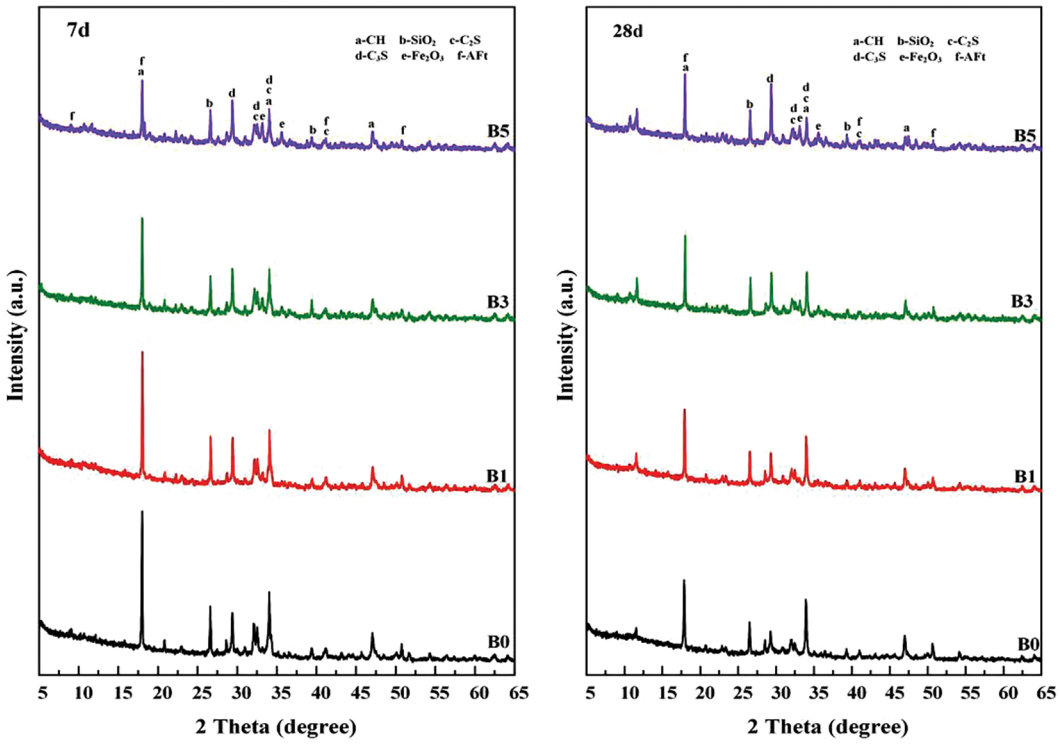


**Figure 7:** Influence of red mud B admixture on the mineral composition of composite mortar after 7 d and 28 d of curing

The microscopic morphologies of the blank specimen B0 and composite specimen B3 at 28 d of age were compared, and the results are shown in Fig. 8. From the microscopic morphology diagram, it can be seen that the composite specimen B3 is denser than the blank specimen B0. Additionally, a significant reduction in large-size pores and an increase in hydration products $Ca(OH)_3$, rod-shaped AFt, and a

denser C-S-H gel were observed, indicating that the incorporation of red mud not only fills the pores and improves the compactness of cement at the early hydration stage but also promotes the hydration of active minerals and improves the mechanical strength of cement [31].

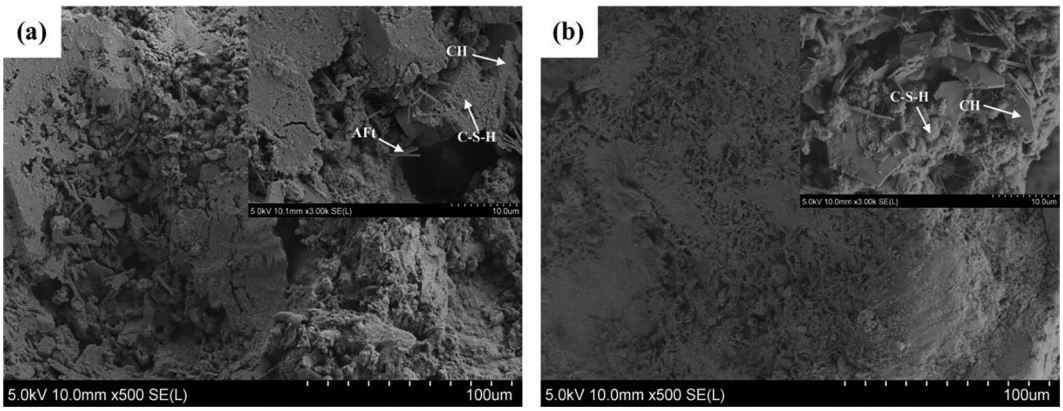


**Figure 8:** Microscopic morphologies of the blank specimen B0 and composite specimen B3 after 28 d of curing

## 4 Conclusions

The following conclusions can be drawn from this study:

(1) As the amount of Bayer red mud increased, the fluidity and initial setting time of the composite mortar gradually decreased, while the final setting time increased. Compared to red mud A, the addition of red mud B resulted in a composite mortar with lower fluidity, a lower initial setting time, and a higher final setting time.

(2) With increasing amounts of red mud A or red mud B, the flexural and compressive strengths of the composite mortar initially increased and then decreased. At a 10 wt% addition of red mud A or a 20 wt% addition of red mud B, the mechanical strength of the composite mortar met the standard requirement for P·O42.5 cement.

(3) The filling and alkali activation effects of Bayer red mud improved the hardness of the hardened mortar and promoted the hydration of active minerals, leading to an increase in the early mechanical strength of the cement stone. However, the weaker activity of Bayer red mud resulted in lower strength of the composite mortar after 28 d of curing.

**Funding Statement:** The authors appreciate the financial support from the Guangxi Science and Technology Program (Guike AD21220052, AD22035126 and AB22035064), National Natural Science Foundation of China (52062009) and Guangxi Key Laboratory of New Energy and Building Energy Saving (Guikeneng 22-J-21-19).

**Conflicts of Interest:** The authors declare that they have no conflicts of interest to report regarding the present study.

## References

1. Wang, P., Liu, D. Y. (2012). Physical and chemical properties of sintering red mud and bayer red mud and the implications for beneficial utilization. *Materials, 5(10),* 1800–1810. https://doi.org/10.3390/ma5101800
2. Zeng, H., Lyu, F., Sun, W., Zhang, H., Wang, L. et al. (2020). Progress on the industrial applications of red mud with a focus on China. *Minerals, 10(9),* 773. https://doi.org/10.3390/min10090773

3. Feng, H., She, X. F., You, X. M., Zhang, G. Q., Wang, J. S. et al. (2022). Carbothermal reduction of red mud for iron extraction and sodium removal. *High Temperature Materials and Processes, 41(1),* 161–171. https://doi.org/10.1515/htmp-2022-0005
4. Venkatesh, C., Nerella, R., Chand, M. S. R. (2020). Experimental investigation of strength, durability, and microstructure of red-mud concrete. *Journal of the Korean Ceramic Society, 57(2),* 167–174. https://doi.org/10.1007/s43207-019-00014-y
5. Khairul, M. A., Zanganeh, J., Moghtaderi, B. (2019). The composition, recycling and utilisation of Bayer red mud. *Resources, Conservation and Recycling, 141(Supplement C),* 483–498. https://doi.org/10.1016/j.resconrec.2018.11.006
6. Liu, Z., Li, H. (2015). Metallurgical process for valuable elements recovery from red mud—A review. *Hydrometallurgy, 155(2–3),* 29–43. https://doi.org/10.1016/j.hydromet.2015.03.018
7. Gray, C. W., Dunham, S. J., Dennis, P. G., Zhao, F. J., McGrath, S. P. (2006). Field evaluation of in situ remediation of a heavy metal contaminated soil using lime and red-mud. *Environmental Pollution, 142(3),* 530–539. https://doi.org/10.1016/j.envpol.2005.10.017
8. Erol, M., Küçükbayrak, S., Ersoy-Mericboyu, A. (2009). The influence of the binder on the properties of sintered glass-ceramics produced from industrial wastes. *Ceramics International, 35(7),* 2609–2617. https://doi.org/10.1016/j.ceramint.2009.02.028
9. Liu, S., Li, Z., Li, Y., Cao, W. (2018). Strength properties of Bayer red mud stabilized by lime-fly ash using orthogonal experiments. *Construction and Building Materials, 166(1),* 554–563. https://doi.org/10.1016/j.conbuildmat.2018.01.186
10. Cao, H., Gao, Q., Zhang, X., Guo, B. (2022). Research progress and development direction of filling cementing materials for filling mining in iron mines of China. *Gels, 8(3),* 192. https://doi.org/10.3390/gels8030192
11. Wang, Y., Liu, X., Li, Y., Li, D., Zhang, W. et al. (2021). Tailings after iron extraction in bayer red mud by biomass reduction: Pozzolanic activity and hydration characteristics. *Materials, 14(14),* 3955. https://doi.org/10.3390/ma14143955
12. Dodoo-Arhin, D., Nuamah, R. A., Agyei-Tuffour, B., Obada, D. O., Yaya, A. (2017). Awaso bauxite red mud-cement based composites: Characterisation for pavement applications. *Case Studies in Construction Materials, 7(1–3),* 45–55. https://doi.org/10.1016/j.cscm.2017.05.003
13. Tian, K., Wang, Y., Dong, B., Fang, G., Xing, F. (2022). Engineering and Micro-properties of alkali-activated slag pastes with Bayer red mud. *Construction and Building Materials, 351(7),* 128869. https://doi.org/10.1016/j.conbuildmat.2022.128869
14. Viyasun, K., Anuradha, R., Thangapandi, K., Kumar, D. S., Sivakrishna, A. et al. (2021). Investigation on performance of red mud based concrete. *Materials Today: Proceedings, 39,* 796–799. https://doi.org/10.1016/j.matpr.2020.09.637
15. Krivenko, P., Kovalchuk, O., Pasko, A., Croymans, T., Hult, M. et al. (2017). Development of alkali activated cements and concrete mixture design with high volumes of red mud. *Construction and Building Materials, 151(4),* 819–826. https://doi.org/10.1016/j.conbuildmat.2017.06.031
16. Ribeiro, D. V., Labrincha, J. A., Morelli, M. R. (2011). Potential use of natural red mud as pozzolan for Portland cement. *Materials Research, 14(1),* 60–66. https://doi.org/10.1590/S1516-14392011005000001
17. Romano, R. C. O., Bernardo, H. M., Maciel, M. H., Pileggi, R. G., Cincotto, M. A. (2018). Hydration of Portland cement with red mud as mineral addition. *Journal of Thermal Analysis and Calorimetry, 131(3),* 2477–2490. https://doi.org/10.1007/s10973-017-6794-2
18. Yang, X., Zhao, J., Li, H., Zhao, P., Chen, Q. (2017). Recycling red mud from the production of aluminium as a red cement-based mortar. *Waste Management & Research, 35(5),* 500–507. https://doi.org/10.1177/0734242X16684386
19. Xu, J., Xu, F., Wu, Y., Liu, Y., Yang, F. et al. (2022). Investigation on properties and mechanism of non-calcined Bayer red mud-phosphogypsum cementitious binder. *Journal of Cleaner Production, 379,* 134661. https://doi.org/10.1016/j.jclepro.2022.134661

20. Ye, N., Chen, Y., Yang, J., Liang, S., Hu, Y. (2016). Co-disposal of MSWI fly ash and Bayer red mud using an one-part geopolymeric system. *Journal of Hazardous Materials, 318,* 70–78. https://doi.org/10.1016/j.jhazmat.2016.06.042
21. Wang, W., Wang, X., Zhu, J., Wang, P., Ma, C. (2013). Experimental investigation and modeling of sulfoaluminate cement preparation using desulfurization gypsum and red mud. *Industrial & Engineering Chemistry Research, 52(3),* 1261–1266. https://doi.org/10.1021/ie301364c
22. Luo, S., Liu, M., Yang, L., Chang, J., Yang, W. et al. (2019). Utilization of waste from alumina industry to produce sustainable cement-based materials. *Construction and Building Materials, 229(1–2),* 116795. https://doi.org/10.1016/j.conbuildmat.2019.116795
23. Ortega, J. M., Cabeza, M., Tenza-Abril, A. J., Real-Herraiz, T., Climent, M. Á. et al. (2019). Effects of red mud addition in the microstructure, durability and mechanical performance of cement mortars. *Applied Sciences, 9(5),* 984. https://doi.org/10.3390/app9050984
24. Chen, R., Cai, G., Dong, X., Mi, D., Puppala, A. et al. (2019). Mechanical properties and micro-mechanism of loess roadbed filling using by-product red mud as a partial alternative. *Construction and Building Materials, 216(2),* 188–201. https://doi.org/10.1016/j.conbuildmat.2019.04.254
25. Venkatesh, C., Nerella, R., Chand, M. S. R. (2021). Role of red mud as a cementing material in concrete: A comprehensive study on durability behavior. *Innovative Infrastructure Solutions, 6(1),* 1–14. https://doi.org/10.1007/s41062-020-00371-2
26. Hong, S. Y., Glasser, F. P. (2002). Alkali sorption by CSH and CASH gels: Part II. Role of alumina. *Cement and Concrete Research, 32(7),* 1101–1111. https://doi.org/10.1016/S0008-8846(02)00753-6
27. Song, S., Zhang, N., Yuan, J., Zhang, Y. (2021). New attempt to produce red mud-iron tailing based alkali-activated mortar: Performance and microstructural characteristics. *Journal of Building Engineering, 43(3–4),* 103222. https://doi.org/10.1016/j.jobe.2021.103222
28. Sousa, M. I. C., Rêgo, J. H. S. (2021). Effect of nanosilica/metakaolin ratio on the calcium alumina silicate hydrate (CASH) formed in ternary cement pastes. *Journal of Building Engineering, 38,* 102226. https://doi.org/10.1016/j.jobe.2021.102226
29. Wang, X., Ma, J., Zhang, L., Yang, J. (2018). Radioactive element distribution characteristics of red mud based field road cement before and after hydration. *Journal of Wuhan University of Technology-Mater. Sci. Ed., 33(2),* 452–458. https://doi.org/10.1007/s11595-018-1844-5
30. Ma, F., Chen, L., Lin, Z., Liu, Z., Zhang, W. et al. (2022). Microstructure and key properties of phosphogypsum-red mud-slag composite cementitious materials. *Materials, 15(17),* 6096. https://doi.org/10.3390/ma15176096
31. Wan, X., Ding, J., Jiao, N., Mou, C., Gao, M. (2022). Mechanical and microstructural properties of cement-treated marine dredged clay with red mud and phosphogypsum. *Bulletin of Engineering Geology and the Environment, 81,* 266. https://doi.org/10.1007/s10064-022-02753-5